Open-source 3D printable frameless stereotaxic system for young and adult pigs

Charles-Henri Malbert

Open-source 3D printable frameless stereotaxic system for young and adult pigs.

Charles-Henri Malbert

Aniscan department, Human nutrition, INRAE, Saint-Gilles, 35590 France

Address for correspondence
Prof Charles-Henri Malbert
Aniscan, INRAE
16 Le clos, 35590 Saint-Gilles, France
charles-henri.malbert@inrae.fr

Abstract

Background: Here we present an open-source solution, comprising several 3D-printable mechanical pieces and software tools, for frameless stereotaxic targeting in young and adult pigs of varying weights.

New method: Localization was achieved using an IR camera and CT imaging. The positions of the tools were followed, after registration of the pig stereotaxic space, with a CT scan and open-source brain atlas. The system was used to target the lateral ventricle and the subthalamic nucleus (STN) in one piglet and two adult Yucatan miniature pigs, which were either normal weight or obese.

Results and conclusions: Positive targeting was confirmed in the first trial for all subjects, either by radiopaque CT enhancement of the ventricle or actual recording of the STN electrophysiological signature. We conclude that open-source freely available models, easily built with low-end 3D printers, and their associated software can be effectively used for brain surgery in pigs, at a minimal cost, irrespective of the weight of the animal.

Keywords: Frameless stereotaxis, Yucatan minipig, ventriculography, subthalamic nucleus, 3D print

Introduction

Pigs are increasingly used in translational research due to their close resemblance to humans (1), (2). Furthermore, miniature porcine breeds provide adult animals easy to handle (3). In addition, the large gyrencephalic brain of the pig enables the use of a clinical scanner without impaired spatial resolution (4). Several digital atlases suitable for brain surgery are available (5), (6), (7), (8), (9), some of which, such as those developed in our laboratory (5), have been published in an open-source format, allowing their incorporation into surgical guidance software (10). Generic and dedicated algorithms are also available to register brains differing in breed, size, and physiological status to these atlases with millimetric accuracy (11), (7). Nevertheless, brain surgery in pigs is complex compared to that in murine models. For example, lateral ventricle cannulation requires head placement in a stereotaxic frame, which is a time-consuming procedure, even for a well-trained surgical team (12). The complexity of the procedure, in part related to the obliquity of the auditory canal (13), has promoted the development of alternate stereotaxic frames, some of which are magnetic resonance imaging (MRI)-compatible (14), (15), (16). These devices allow precise targeting at the expense of the time required for co-registration of the frame relative to the scanner and to the atlas three-dimensional (3D) spaces. However, they are not suitable for obese adult miniature pigs weighing ≥ 100 kg as the development of the adipose tissue enlarges the head; this is an important limitation considering the use of the pig as a model for human obesity (17). Furthermore, these devices were adequately suited for young animal skulls with parietal and frontal bones parallel to the palate. This was not the case in adult animals for which the brain forms a 50° angle with the palate (4), rendering it difficult to target with a Horsley–Clarke or Leksell frame.

The past decade has seen a shift toward frameless guidance technologies for human neurosurgical procedures as these platforms are lighter, smaller, and easier to use than the more classical stereotaxic frames (18). Unfortunately, these tools are dedicated to humans, and the mandatory software required for targeting is devoted to the human atlas (19). Furthermore, the human brain is three times larger than the porcine brain, rendering these platforms too big to be applied to the pig skull. In addition, the cost of these platforms and the difficulties in interoperating tools from different suppliers led to difficulty with the translation. With the development of affordable 3D printers, we believe

that all of these limitations can be overcome using open-source hardware and software dedicated to porcine brain surgery. The availability of these tools is likely to promote porcine brain surgery in a similar way as our freely accessible porcine atlas, which is used far beyond in-house research (20), (21), (9), (22).

This study aimed to develop and validate an open-source set of tools combining software and hardware components suitable for stereotaxic placement of catheters or electrodes within the brains of adult and growing pigs, irrespective of their weight. The system used a commercially available 3D localizer infrared (IR) camera for precise positioning. The localizer was the only piece of hardware that was not open-source or 3D printable. Each of the tools supporting four reflective markers is capable of sub-millimeter accuracy. The system takes advantage of CustusX software (23), an open-source software designed by the Norwegian National Competence Center for ultrasound and image-guided therapy. The software processes online data from the infrared localizer and overlaps them with the models describing the porcine brain and stereotaxic supports. Our system was primarily oriented for the placement of ventricular catheters and push-pull cannulas that do not require accurate positioning. It was further challenged by targeting a smaller zone, which requires precise navigation capabilities. The subthalamic nucleus (STN) was chosen because it is difficult to access and exhibits a specific electrophysiological signature even in anesthetized animals (4). All software and hardware tools constituting the stereotaxic system are described in Supplemental Material 1. The hardware tools were designed to be easily printable using an entry-level 3D printer.

Materials and methods

1. Animals & ethical considerations

Three animals were used for the experiment: one growing large white piglet (young) weighing 32 kg and aged 3 months, one adult miniature Yucatan pig weighing 45 kg (adult), and one adult miniature obese Yucatan pig weighing 85 kg (obese), both aged 2 years. All of the included animals were female and cover the weight span used in porcine experimental brain surgery. The young animal could be fitted in a classical stereotaxic frame (13), (4), but the adult animal required a stereotaxic box on which the metal frame itself was attached (24). The obese animal was unsuitable for any published stereotaxic apparatus due to fattening of the neck. Obesity was induced in the obese animal using the protocol described by Malbert et al. (17). All animals were euthanized at the end of the surgical procedure. The experiment was conducted in accordance with the current ethical standards of European legislation after validation by the ethic committee of Rennes (2015102913338236).

2. Anesthesia

The experiment was performed under general anesthesia using local and systemic pain suppression protocols. During the entire procedure, including CT imaging, the animals were placed in ventral recumbency with their head stabilized by an air-tight cushion containing polyethylene marbles (Vacuform Silplus; Schmidt, Garbsen, Germany). General anesthesia was achieved using sevoflurane (Baxter, Maurepas, France) about 2.5 % v/v, delivered by a positive pressure ventilator (AS/3; General Electric, Milwaukee, USA) connected to an endotracheal tube inserted after sedation with ketamine (Imalgene, Merial, Lyon, France, 5 mg/kg, IM). Fentanyl was delivered intravenously using a syringe driver over the course of the procedure (0.4 µg/kg/min minimum, Fentadon; Dechra, Montigny le Bretonneux, France). Increases in the heart rate or blood pressure during potentially painful stimulation were monitored together with spO_2/$spCO_2$ (ADU 3; General Electric, Milwaukee, USA) and used to modulate the rate of delivery of fentanyl. The ventilator settings were selected to lower the $spCO_2$ to 3% v/v, while maintaining spO_2 at ≥ 98% to reduce cerebral blood flow and intracranial pressure (25). In addition, subcutaneous and periosteal injections of lignocaine 10% (2–3 ml; Aguettant, Lyon, France) were administered before the onset of the craniotomy and

repeated every 90 min. A hot-air heating blanket (3M Bair Hugger; Cergy-Pontoise, France) was placed over the animal to maintain homeothermy.

3. Frameless tools

Several tools were designed to facilitate the insertion and positioning of the cannula guide (Figure 1, Supplemental Material 1). All of the tools were based on a ball within a cup concept that included *a minima*, a female frame screwed on the skull while centered on the burr hole, and a rotating mobile piece for cannula guidance. This design extended a more complex design by Sudhakar et al. for non-human primates (18). The mobile piece was squeezed by a large screw attached to the swivel base, which could be replaced by a screw serving as a cap for longer experiments. Several mobile pieces were designed with different holding sub-units to fit different cannula sizes, including an adjustable chuck to maintain the cannula in place without metal screws, which could otherwise create artifacts on CT images. This mobile piece was tested for cannula placement in the lateral ventricle. The most complex mobile piece was used to target the subthalamic nucleus; this piece included a stepper motor and was used for the robotic placement of the recording electrodes. We selected a robotic solution because (i) the mobile descender was too flexible for direct manual descent, and (ii) this solution allowed continuous artifact-free recording during targeting. The motor was controlled by an external rotary encoder placed on a remote controller box to avoid any contact between the surgeon and the mobile piece. The connection schematic and the software used by the Arduino controller (Arduino cc, Italy) are described in Supplemental Material 1. The software was written in such a way that one turn of the encoder resulted in a 50 µm travel along the electrode axis. The robotic system was designed to accommodate a StarFix stereotaxic microelectrode with an insertion tube (FHC, USA). The quality of the power supply is important for artifact-free recording of a single neuronal unit. Several types of power supplies were tested, and an adequate supply was provided by the A/D converter box used for electrophysiological recordings (Analog Discovery 2; Digilent, Pullman, USA) that delivered a noise-free DC. Furthermore, this configuration allowed electrical insulation from the mains once the laptop was running on the battery. The preamplifier was built around an AD 8232 integrated analog front end (Analog Devices, Wilmington, USA) enclosed in a shielded miniature box placed close to the skull. This device has already been successfully used for DBS recordings (26). Details about the construction of the

actual preamplifier and its performance are given in Supplemental Material 2. The connections between the electronic boards, electrode, and robotic descender are presented in Supplemental Material 3.

Figure 1

The tools were designed using RhinoCeros software (V7; Robert McNeel and Associates, USA), converted to STL format, and sliced with Ultimaker Cura software (V4.8.0; Ultimaker B.V.) for final printing. These tools were ultimately printed on an Ender pro 3 printer (Creality3D, Shenzhen, China) with a PLA+ (polylactic acid) wire. The sensitivity of the IR camera to light scattering required that the printing material was made of black filament. Details about the printing parameters, number of individual pieces required, and printing sequence are given in Supplemental Material 1.

4. Localizer tools

The localizer tools were tracked by a Polaris Spectra (NDI, Waterloo, Canada) that was located approximately 1.5 m above the surgical plane and attached to a Macintosh computer running CustusX software. Three localizer tools were designed with two reference frames. The schematic for the distance and angle between the reflective markers was obtained from the Apple library created under an open-source license by Brown et al. (27). This library allowed several localizers to simultaneously track whether their ROM definitions (the file format used by the NDI localizer) were inserted into the navigation software. One tool (the cannula tool) consisted of a stainless steel rod (2 mm OD; Phymep, Paris, France) attached to a localizer frame. The diameter of the rod was selected such that it could be inserted into a 2.85 mm OD stainless steel tube that served for ventricular access or to attach an additional smaller tube to create a push-pull cannula. The rod outer end was tightly inserted in Luer to 1/4 28 female peek adapters (Idex Health and Science, Oak Harbor, USA) to allow connection with a Luer-tipped syringe. The inner end, designed to be inserted into the brain, was carefully polished with a rotating felt brush under binocular conditions. Another tool (the coagulator tool) accommodated a coagulation electrode (Dixi Medical, Chaudefontaine, France), and the last localizer was designed to be attached to the robotic targeting device. For each tool, a ROM definition was constructed from scratch using NDI Architect software (V6; NDI, Waterloo, Canada) together with the required .xml files to be inserted into the CustusX

navigation software. The two reference frames had identical distances and angles between the reflective markers and were attached to dissimilar supports. One frame was used during the initial navigation steps and was placed under the chin of the animal. The second frame could be adjusted in any direction and was designed such that its end was fixed directly on the skull. As the references were virtually identical for the navigation software, it was possible to exchange them during surgery to optimize their IR camera visibility. NDI tracker software (NDI V5.001, Waterloo, Canada) was used as the first step of the surgical procedure to confirm the visibility of the tools and optimize the position of the NDI camera.

5. Software customization

CustusX software (https://www.custusx.org) was customized to allow 3D localization of the coagulator, cannula, and motorized targeting tools. Several files including ROM definitions have been designed and are available in the “Tools definition for Custus X” folder of Supplemental Material 1. Once detected by the IR camera, the tool was displayed on a real-time screen using a simplified 3D representation (included with each tool). While the ROM files were immediately usable, it is advisable to “pivot” the tool using the pivoting procedure described in the NDI Architect software to update the ROM file; this compensates for small variations in the length of the bar/coagulator.

VTK and STL models of the pig brain ventricles and each of the tools plus the swivel base are provided in the Supplemental Material. The biological models were obtained from the conversion in VTK format, using 3D Slicer software (V4.10.2, https://www.slicer.org) (28) of the pig brain atlas developed in our laboratory (5). The software models were required to be uploaded to CustusX before the registration procedure for a comprehensive representation of the surgical scene (Figure 2).

Figure 2

6. CT imaging

CT imaging was performed with the animals in ventral recumbency using either a HiSpeed NX:i or a Discovery ST PET/CT (General Electric, Milwaukee WI, USA). Data collection was achieved in helicoidal mode (120 kV, 100–200 mA, depending on the scout scan, with a section thickness of 1 mm). A minimum of two scans was achieved per

animal - the first one after the placement of the external references on the skin, and the second one once the targeting was completed. The first scan also served to calculate the skull bone thickness and was part of a failsafe procedure to position a drill guard (details of construction are described in Supplemental Material 1) on the burr-hole drill. The second scan confirmed the placement of the cannula in the lateral ventricle after the injection of 2 ml radio-opaque medium (Hexabrix 320, Guerbet, Villepinte, France). After completion, the images were transferred from the CT scanner to the Osirix reader (29), and ultimately imported into Dicom format to CustusX.

Results

The sequential steps required for adequate targeting are shown in Figure 3. The steps were completed in < 30 min for the ventriculography and 45 min for the STN recording, irrespective of the age and weight of the animal.

Figure 3

Positioning

While the external reference chips (for construction, see Supplementary Materials) were initially planned to be stitched to the skin, fixing was difficult in adult miniature pigs due to the hardness of their skin. Therefore, these references were maintained using surgical glue (Vetbond, 3M; Cergy-Pontoise, France) as a rapid and effective alternative. Registration between the anatomical and real-world spaces was performed by pinpointing each of the skin's external references with the coagulator tool (steps 7 and 11, Figure 3). Virtual targeting was achieved with the coagulator tool before skin opening using the virtual tooltip offset option in CustusX. This step was mandatory given that access to the cerebral target could be limited depending on the skull thickness and the target location (Figure 4).

Figure 4

The precise location of the burr hole was achieved after skin opening using a coagulation current applied on the coagulator tool, which resulted in a dark spot on the skull. Creation of the burr hole down to the dura matter was impossible in the adult miniature pig using “smart” cranial perforators because the distance between the two cortical layers of the skull was too large, i.e., above the 1.5 mm requirement. Indeed, the thickness of the adult skull range from 29–35 mm depending on the planned location of the burr hole. Blocking the unlocking system with one drop of cyanoacrylate superglue was sufficient to gain additional perforating thickness capability and complete dura matter access. Dura matter opening was achieved by applying a coagulation waveform current on the coagulator tool. Once the brain's surface was made accessible, a dummy swivel base, including three screws, was positioned over the outside hole. The planned location of the holes used on the skull for screw fixation was marked with coagulator current directly applied on the screws. The final swivel base was then fixed firmly on the

skull and the mobile part was inserted and secured.

Ventriculography

Ventricular access was performed using the cannula tool, that is, the cannula was fitted with a slightly longer stainless rod supporting the localizer. A second registration was performed using the external references and two of the three screws that maintained the swivel base. Using a Polaris Spectra 1.5 m from the skull, the accuracy was less than the millimeter range using the third screw of the swivel base as a test point. Afterwards, the entire cannula system was inserted approximately 20 mm such that its tip did not protrude the mobile piece and an adequate angle was found. The tightening screen was firmly set, and the cannula was slowly inserted using CustusX clues. Once at the correct location, the guide rod was removed, the cannula was fixed, and the Luer-lock matting connector was placed on the cannula. Correct placement of the cannula was confirmed by positive ventricular radio marking (Figure 5); placement was successful in all animals after the first descent.

Figure 5

STN targeting

STN targeting was achieved after ventriculography and replacement of the mobile cannula guide by the robotic mobile piece without the need to drill an additional burr hole. The electrode guide with rigidifying rod was inserted rapidly, such that the electrode tip was in the thalamus once in the guide. The rigid internal rod was then removed and replaced with an actual electrode. After adequate grounding was achieved by running the laptop on the battery, the thalamic activity was immediately recorded as irregular large-amplitude spikes. The descend was resumed in 100 µm steps until a sustained activity was collected, indicative of the STN entrance. This activity was recorded continuously over 3.5–4 mm, depending on the animal. Spiking became sparse when the electrode was excited from the STN, indicative of substantia nigra neuronal activity (Figure 6).

Figure 6

Discussion

To the best of our knowledge, this study represents the first demonstration of easy access to the lateral ventricle and deep brain structures in an adult obese miniature pig using a complete frameless stereotaxic system suitable for 3D printing. While commercial frameless systems are available, they are costly and designed primarily for human surgery, making them poorly suited for porcine studies. Furthermore, their software are purposely trademarked tools that are locked with human atlases. These limitations were overcome by our open-source design, which was easily assembled using an entry-level 3D printer.

Our initial goal was to create a system for easy access to large brain structures, irrespective of the age and weight of the animal. While precise, the classic stereotaxic apparatus requires complex and time-consuming adjustments of the head relative to the frame. One of the most demanding processes was to achieve symmetrical positioning of the head relative to the frame. Although the localizer box designed by the Bjarkam group (24), (15) represented a step forward, with increased simplicity without an impaired resolution, the duration of the placement remained an issue. Because the ventricle is a large structure, a reduced spatial resolution was acceptable at the expense of the duration of the procedure. A more complex placement, for example, STN targeting, was also possible using a robotic mobile tool. The increased accuracy needed for STN targeting was partly due to sequential registration using skin references and their subsequent partial substitution by the screws used to fix the swivel base. The uneven placement of the fixation holes on the base side was another reason for this increased accuracy.

Some tools were relatively straightforward to build, while others required maximal resolution of the printer and the activation of special printing options. Moreover, all of the tools were built with PLA+ plastic, which are known to become fragile with time when placed in a wet environment. One swivel base was built for each pig because during the *in vitro* tests, one of the three flanges constituting the receiving cup was partially broken upon successive insertion/removal of the mobile piece. Aside from this sensitive piece, the remaining tools were identical between animals, and all were immersed in sterilization liquid (glutaraldehyde 2%; Steranios, Anios, Lille, France) without further problems. The robotic mobile piece was not sterilized because the stepper motor was not

waterproof. One swivel base and its matting occluding screw were printed in ABS (Acrylonitrile butadiene styrene), a waterproof and improved ductility plastic. The printing process was not a significant issue despite the increased temperature required for ABS filament fusion, demonstrating that the STL models were suitable for both thermoplastics irrespective of their heat-shrinking coefficients.

One limitation of the frameless system was the absolute requirement to maintain both the reference frame and active tool insight for the infrared camera. As the surgery was supposed to be performed directly on the CT table, the bulk of the CT enclosure prevented the location of the camera by approximately 180° (either frontal or dorsal to the animal, depending on the surgeon's lateral preferences). Even with the maximal height between the surgical area and the camera, this limitation reduced the visibility of the reference frame, especially if positioned close to the chin. Two supports dedicated to the reference frame were designed in an attempt to minimize this issue. Nevertheless, the surgeon must take care when performing the actual acquisition of both the active and reference frames, especially during the descent of the cannula. Fortunately, flags present on the main screen of the CustusX software consistently indicated the effectiveness of the tracking. The physical balance of the tools in the surgeon’s hand is another important issue for the simplicity of the procedure. While several attachment possibilities were incorporated in the design by Sudhakar et al. (18), the most suitable for adequate balance was selected. Care must be taken when assembling the tools to match the correct holes because the ROM files are designed for a specific attachment only.

The difficulties in accessing the cortical surface of adult pigs cannot be underestimated. First, the distance between the two cortical layers of the skull is larger than the limit claimed by “smart” drill supplier; this prevents the use of the clutch mechanism, which is supposed to act as a failsafe device for preventing dura mater damage. Conversely, removing the clutch mechanism required adding a movable ring on the outside of the drill as a substitute. However, even when the hole was made, the accessibility of the dura mater was poor, impeding the use of a dedicated hook to lift the membrane. The use of a navigable coagulator tool was an alternative for opening the dura mater, but it was the most challenging surgical gesture of the entire procedure. The use of a navigable coagulator tool could be made less challenging by using surgical grade magnifier goggles and an additional focused light source.

It was possible to estimate the system's targeting possibilities with specific reference to the target depth and thickness of the skull. Unsurprisingly, the target possibilities increased linearly with the target depth. Nevertheless, deeply located targets are more complex to reach because the system's offsetting capability halves when the skull thickness triples, that is, when a piglet becomes adult. Knowing that the encephalon fit within a box approximately 60 × 40 × 35 mm (5), the entire brain is not accessible with a single burr hole. This explains the importance of surgical planning and the need for the swivel base to have a precise location.

The system described here resembles the StealthStation surgical navigation system (Medtronic, Minneapolis, USA); the StealthStation is restricted to use in humans because the navigation software does not allow the insertion of alternative atlases (30). Furthermore, the commercial skull-mounted trajectory guide is twice as large as our design given the space available on the human skull, and is therefore unsuitable for the porcine brain. Although pigs have a sizeable skull, they exhibit limited projection surfaces that are suitable for positioning a guide, which prevents the placement of the StealthNavigus guide or alternative commercial guides such as the Monteris Axiis. The size of the swivel base (45 mm), dictated by the diameter of the burr hole, was probably the maximal acceptable size, knowing that the skull's maximal usable width was 65 mm. The size was also an obstacle to the deployment of an MRI-compatible platform, such as the NextFrame device (31) or the SmartFrame (32). Finally, the brainsight neuronavigator allowed custom implant design but required dedicated surgical tools, resulting in a practical but costly solution that is yet to be published in pigs (33). The advantages and disadvantages of these systems are listed in Table 1.

Table 1

The addition of an electromagnetic localizer at the tip of the cannula represent an exciting addition to the IR localization. However, it is important to balance the system's increased complexity, cost, and easiness for targeting large structures such as the ventricle. While a waterproof stepper may be useful, the price tag for a miniature waterproof stepper is significant. The most relevant improvement is probably a simplification of the CustusX user interface and its dedication to brain navigation only. The open-source code is highly versatile, including hybrid representation with synchronization of CT based images, ultrasound video, and ultrasound 3D reconstruction.

Several registration methods, which are mandatory for the initial purpose of the software, e.g., bronchoscopy, also contributed to the complexity of the interface (23). The alternative open-source navigation software, 3D Slicer, with the adequate registration plugin, was powerful but equally complex (28).

In conclusion, we describe an open-source 3D printable frameless stereotaxic system that is suitable for both adult and young pigs, irrespective of their weight. This system was not designed to replace the already developed frame-based stereotaxic apparatus, but as an effective substitute for rapid and easy probe placement within sub-millimetric targets. While it was tested for ventricular access and recording of STN activity, the system is suitably flexible for radiofrequency lesioning or excitotoxin injections using an optimal path to the desired target (34). The technique and instrumentation may benefit future research within this species, and was designed to be easily duplicated with a low-cost 3D printer using the models supplied.

Conflicts of Interest: The author declares no conflict of interest

Acknowledgement: The author thanks staff of the UE3P unit for animal care, Alain Chauvin, Mickael Genissel, Julien Georges and Francis Le Gouevec. We also thank Jean-François Rouault for the production of the experimental diets.

Disclosure Statement and competing interests: The authors have no conflicts of interest to declare.

Guarantor's statement: Charles-Henri Malbert is the guarantor of this work and, as such, had full access to all the data in the study and takes responsibility for the integrity of the data and the accuracy of the data analysis.

Funding sources - The study was conducted with the support of INRAE.

Authors' contribution - C-H.M. planned the experiments, conducted the studies, analyzed the data, and was responsible for writing the manuscript.

References

1. Malbert C-H: [The brain-gut axis: insights from the obese pig model]. *Bulletin de l'academie nationale de medecine* 197:1683-1694, 2013

2. Bech J, Orlowski D, Glud AN, Dyrby TB, Sørensen JCH, Bjarkam CR: Ex vivo diffusion-weighted MRI tractography of the Göttingen minipig limbic system. *Brain Struct Funct* 225:1055-1071, 2020

3. Malbert C-H: Vagally Mediated Gut-Brain Relationships in Appetite Control-Insights from Porcine Studies. *Nutrients* 13:467-484, 2021

4. Sauleau P, Lapouble E, Val-Laillet D, Malbert CH: The pig model in brain imaging and neurosurgery. *Animal* 3:1138-1151, 2009

5. Saikali S, Meurice P, Sauleau P, Eliat PA, Bellaud P, Randuineau G, Vérin M, Malbert CH: A three-dimensional digital segmented and deformable brain atlas of the domestic pig. *J Neurosci Methods* 192:102-109, 2010

6. Conrad MS, Dilger RN, Johnson RW: Brain growth of the domestic pig (Sus scrofa) from 2 to 24 weeks of age: a longitudinal MRI study. *Developmental neuroscience* 34:291-298, 2012

7. Villadsen J, Hansen HD, Jørgensen LM, Keller SH, Andersen FL, Petersen IN, Knudsen GM, Svarer C: Automatic delineation of brain regions on MRI and PET images from the pig. *J Neurosci Methods* 294:51-58, 2018

8. Orlowski D, Glud AN, Palomero-Galagher N, Sørensen JCH, Bjarkam CR: Online histological atlas of the Göttingen minipig brain. *Heliyon* 5:e01363, 2019

9. Chang SJ, Santamaria AJ, Sanchez FJ, Villamil LM, Pinheiro Saraiva P, Rodriguez J, Nunez-Gomez Y, Opris I, Solano JP, Guest JD, Noga BR: In vivo Population Averaged Stereotaxic T2w MRI Brain Template for the Adult Yucatan Micropig. *Front Neuroanat* 14:599701, 2020

10. Malbert C-H: AniMate-An open source software for absolute PET quantification. Annual congress of the european association of nuclear medicine 43:np, 2016

11. Vállez Garcia D, Casteels C, Schwarz AJ, Dierckx RA, Koole M, Doorduin J: A standardized method for the construction of tracer specific PET and SPECT rat brain templates: validation and implementation of a toolbox. *PLoS One* 10:e0122363, 2015

12. van Eerdenburg FJCM, Dierx JAJ: A new technique for long term, stress free, cannulation of the lateral ventricle in postpubertal, freely moving, pigs. *Journal of neuroscience methods* 121:13-20, 2002

13. Marcilloux J-C, Rampin O, Felix M-B, Laplace J-P, Albe-Fessard D: A stereotaxic apparatus for the study of the central nervous structures in the pig. *Brain research bulletin* 22:591-597, 1989

14. Bjarkam CR, Cancian G, Larsen M, Rosendahl F, Ettrup KS, Zeidler D, Blankholm AD, Østergaard L, Sunde N, Sørensen JC: A MRI-compatible stereotaxic localizer box enables high-precision stereotaxic procedures in pigs. *J Neurosci Methods* 139:293-298, 2004

15. Bjarkam CR, Cancian G, Glud AN, Ettrup KS, Jørgensen RL, Sørensen J-C: MRI-guided stereotaxic targeting in pigs based on a stereotaxic localizer box fitted with an isocentric frame and use of SurgiPlan computer-planning software. *Journal of neuroscience methods* 183:119-126, 2009

16. Edwards CA, Rusheen AE, Oh Y, Paek SB, Jacobs J, Lee KH, Dennis KD, Bennet KE, Kouzani AZ, Lee KH, Goerss SJ: A novel re-attachable stereotactic frame for MRI-guided neuronavigation and its validation in a large animal and human cadaver model. *J Neural Eng* 15:066003, 2018

17. Malbert C-H, Picq C, Divoux J-L, Henry C, Horowitz M: Obesity-associated alterations in glucose metabolism are reversed by chronic bilateral stimulation of the abdominal vagus nerve. *Diabetes* 66:848-857, 2017

18. Sudhakar V, Mahmoodi A, Bringas JR, Naidoo J, Kells A, Samaranch L, Fiandaca MS, Bankiewicz KS: Development of a novel frameless skull-mounted ball-joint guide array for use in image-guided neurosurgery. *J Neurosurg* 132:595-604, 2019

19. Takenaka T, Toyota S, Kuroda H, Kobayashi M, Kumagai T, Mori K, Taki T: Freehand Technique of an Electromagnetic Navigation System Emitter to Avoid Interference Caused by Metal Neurosurgical Instruments. *World Neurosurg* 118:143-147, 2018

20. Slopsema JP, Canna A, Uchenik M, Lehto LJ, Krieg J, Wilmerding L, Koski DM, Kobayashi N, Dao J, Blumenfeld M, Filip P, Min HK, Mangia S, Johnson MD, Michaeli S: Orientation-selective and directional deep brain stimulation in swine assessed by functional MRI at 3T. *Neuroimage* 224:117357, 2021

21. Fang X, Sun W, Jeon J, Azain M, Kinder H, Ahn J, Chung HC, Mote RS, Filipov NM, Zhao Q, Rayalam S, Park HJ: Perinatal Docosahexaenoic Acid Supplementation Improves Cognition and Alters Brain Functional Organization in Piglets. *Nutrients* 122020

22. Cho S, Min HK, In MH, Jo HJ: Multivariate pattern classification on BOLD activation pattern induced by deep brain stimulation in motor, associative, and limbic brain networks. *Sci Rep* 10:7528, 2020

23. Askeland C, Solberg OV, Bakeng JBL, Reinertsen I, Tangen GA, Hofstad EF, Iversen DH, Våpenstad C, Selbekk T, Langø T, Hernes TAN, Olav Leira H, Unsgård G, Lindseth F: CustusX: an open-source research platform for image-guided therapy. *International Journal of Computer Assisted Radiology and Surgery* 11:505-519, 2016

24. Bjarkam C: A MRI-compatible stereotaxic localizer box enables high-precision stereotaxic procedures in pigs. *Journal of Neuroscience Methods* 139:293-298, 2004

25. Ramina R, Aguiar PHP, Tatagiba M: Samii's Essentials in Neurosurgery. 382, 2007

26. Parastarfeizabadi M, Kouzani AZ, Beckinghausen J, Lin T, Sillitoe RV: A Programmable Multi-biomarker Neural Sensor for Closed-loop DBS. *IEEE Access* 7:230-244, 2018

27. Brown A, Uneri A, Silva T, Manbachi A, Siewerdsen JH: Design and validation of an open-source library of dynamic reference frames for research and education in optical tracking. *J Med Imaging (Bellingham)* 5:021215, 2018

28. Fedorov A, Beichel R, Kalpathy-Cramer J, Finet J, Fillion-Robin JC, Pujol S, Bauer C, Jennings D, Fennessy F, Sonka M, Buatti J, Aylward S, Miller JV, Pieper S, Kikinis R: 3D Slicer as an image computing platform for the Quantitative Imaging Network. *Magn Reson Imaging* 30:1323-1341, 2012

29. Rosset A, Spadola L, Ratib O: OsiriX: an open-source software for navigating in multidimensional DICOM images. *J Digit Imaging* 17:205-216, 2004

30. Palys V, Holloway KL: Frameless Functional Stereotactic Approaches. *Prog Neurol Surg* 33:168-186, 2018

31. Mazzone P, Stefani A, Viselli F, Scarnati E: Frameless Stereotaxis for Subthalamic Nucleus Deep Brain Stimulation: An Innovative Method for the Direct Visualization of Electrode Implantation by Intraoperative X-ray Control. *Brain Sciences* 8:90, 2018

32. Larson PS, Starr PA, Bates G, Tansey L, Richardson RM, Martin AJ: An Optimized System for Interventional Magnetic Resonance Imaging-Guided Stereotactic Surgery: Preliminary Evaluation of Targeting Accuracy. *Operative Neurosurgery* 70:ons95-ons103, 2012

33. Ortiz-Rios M, Haag M, Balezeau F, Frey S, Thiele A, Murphy K, Schmid MC: Improved methods for MRI-compatible implants in nonhuman primates. *J Neurosci Methods* 308:377-389, 2018

34. Frey S, Comeau R, Hynes B, Mackey S, Petrides M: Frameless stereotaxy in the nonhuman primate. *Neuroimage* 23:1226-1234, 2004

Figure 1. Frameless swivel and base in 3D representation (A) and location (B) fixed on an adult obese minipig. Note the thickness of the skin. The sizes indicated in (C) are in mm. (D) Actual presentation of the tools used in the frameless system (the robotic mobile piece is not shown). 1. Reference frame to be placed under the chin. 1bis. Reference frame to be fixed on the skull at a distance from the burr hole. 2 Cannula tool with stop ring. 3 Coagulator tool. 4. Mobile guide. 5. Swivel base. 6. Swivel locking screw.

Figure 2. Actual procedure for ventriculography in an adult obese Yucatan miniature pig weighing 85 kg. (A) Position of the external reference markers on the skin and their registration with the CT counterpart. (B) Descent of the cannula tool. The cannula tool is depicted as a conical grey marker, the swivel base and mobile cannula holder are in green, the target is in red, and the cannula path is presented as a thin green line. The animal was placed in a non-symmetrical manner with the head slightly tilted to investigate the capability of the system to work with suboptimal positioning relative to the CT plane.

Figure 3. Flowchart of the surgical procedure used to access the lateral ventricle or to record the neuronal activity from the STN. The red structure corresponds to the ventricular model. Note the green numbers/dots used for registration between the anatomical model and real-world space. The first insert was obtained with the NDI tracking software.

Figure 4. Reconstruction of the theoretical volume (light blue) that can be explored after insertion of the frameless tool either in a piglet (left panel) or an adult miniature pig (right panel). The outlines of the skull were obtained after thresholding, projection of the actual CT images using Osirix, and further importation in Rhino Software. The contours of the brain were obtained from our pig brain atlas (5), and were coregistered using 3D slicer with the actual CT volume of the brain. A small gap between the brain and the skull reconstructions was introduced in the rendering to ease visualization. The diameter of the burr hole corresponded to the largest available drill from the surgical suppliers. The arrows indicate the sinuses. Note, in the adult pig, the posterior extension of the frontal sinuses engulfing the dorsal projection of the parietal and temporal cortices.

Figure 5. Cannula positioned for ventriculography and radio-opaque underlining the left lateral ventricle.

Figure 6. (A) Robotic tool for electrode insertion in a deep target such as the subthalamic nucleus (STN). The device includes a stepper motor the electronic control of which is

described in the Supplemental Material. The mobile element is designed to accommodate the guide tube of an FHC bipolar concentric electrode. (B) Extracellular recordings of the neuronal activity recorded during the descent of the electrode. The electrode path was selected to encounter, in sequence, the thalamus (a), the STN (b), and the substancia nigra (c). The middle traces are representative of STN neurons, the first trace is representative of thalamic neurons, and the last trace corresponds to the substancia nigra. The quiescent recording periods of transitioning between structures are not shown.

A

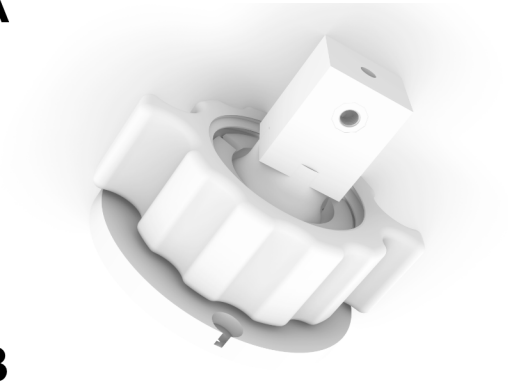

B

C

D

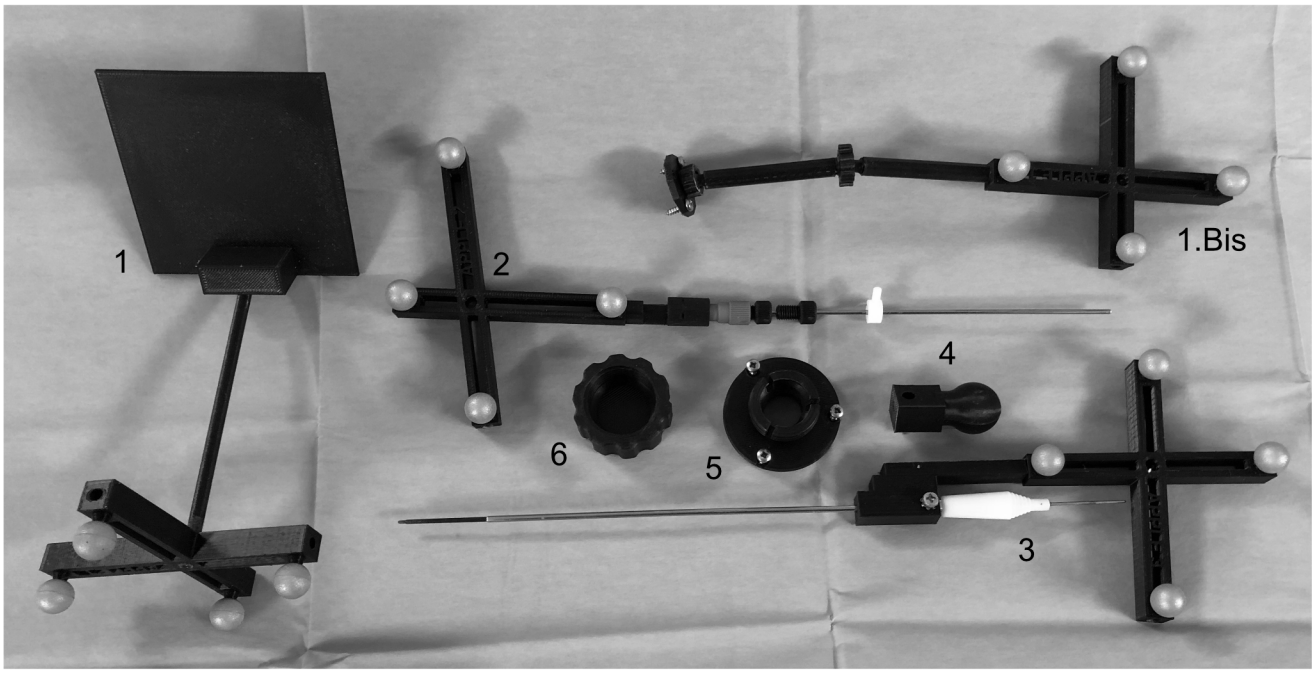

A

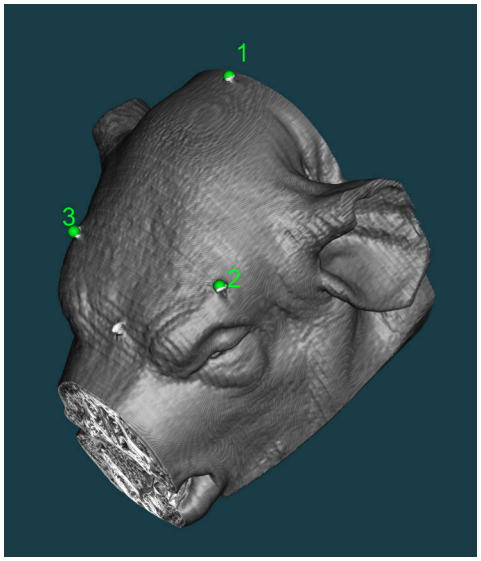

B

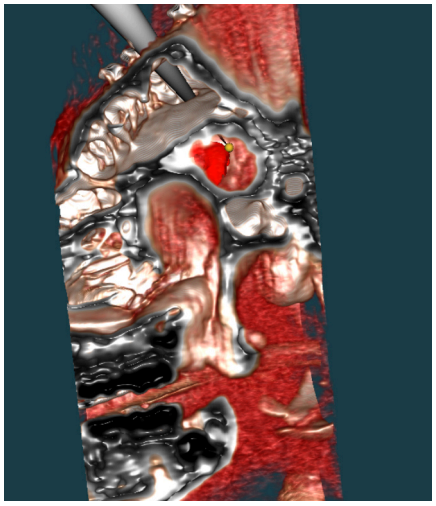

C

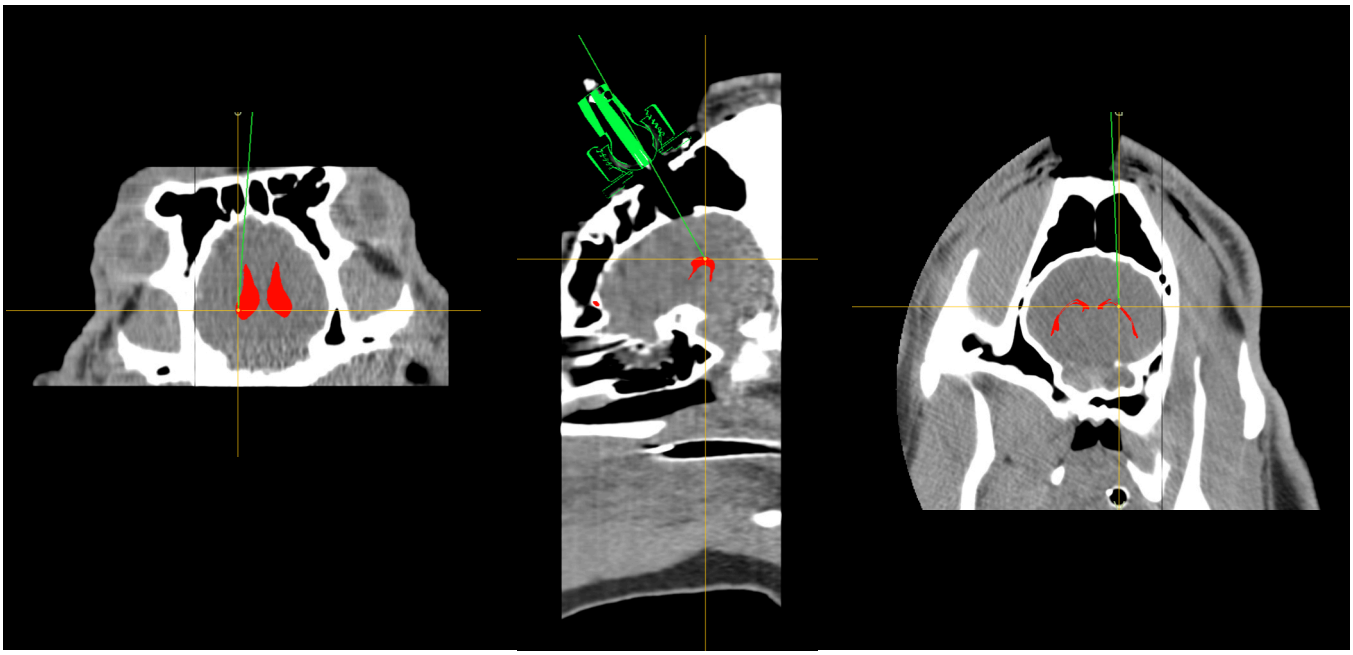

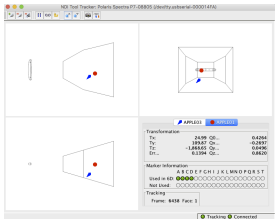

Position reference tool under the chin

Check scan volume within localiser range

Position external markers n= 4

CT scan (1 mm slice)

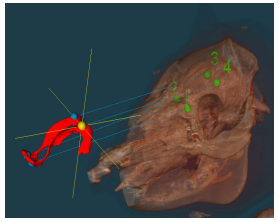

Import CT to CustusX

Import VTK model and co-register

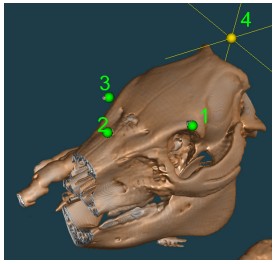

Register volume to real world using coagulator tool

Burr hole and opening of dura matter using coagulator tool

Fix swivel on the skull

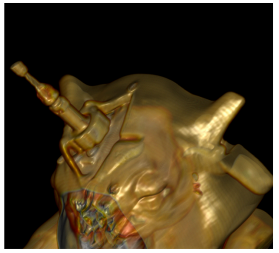

Insert ball guide in swivel

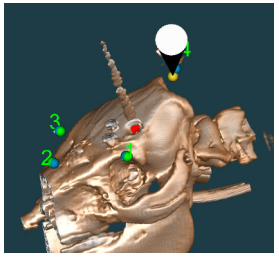

Register volume to real world using cannula tool

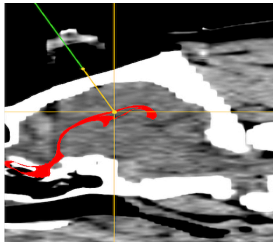

Guide cannula tool to target using Custus X 'extend' feature

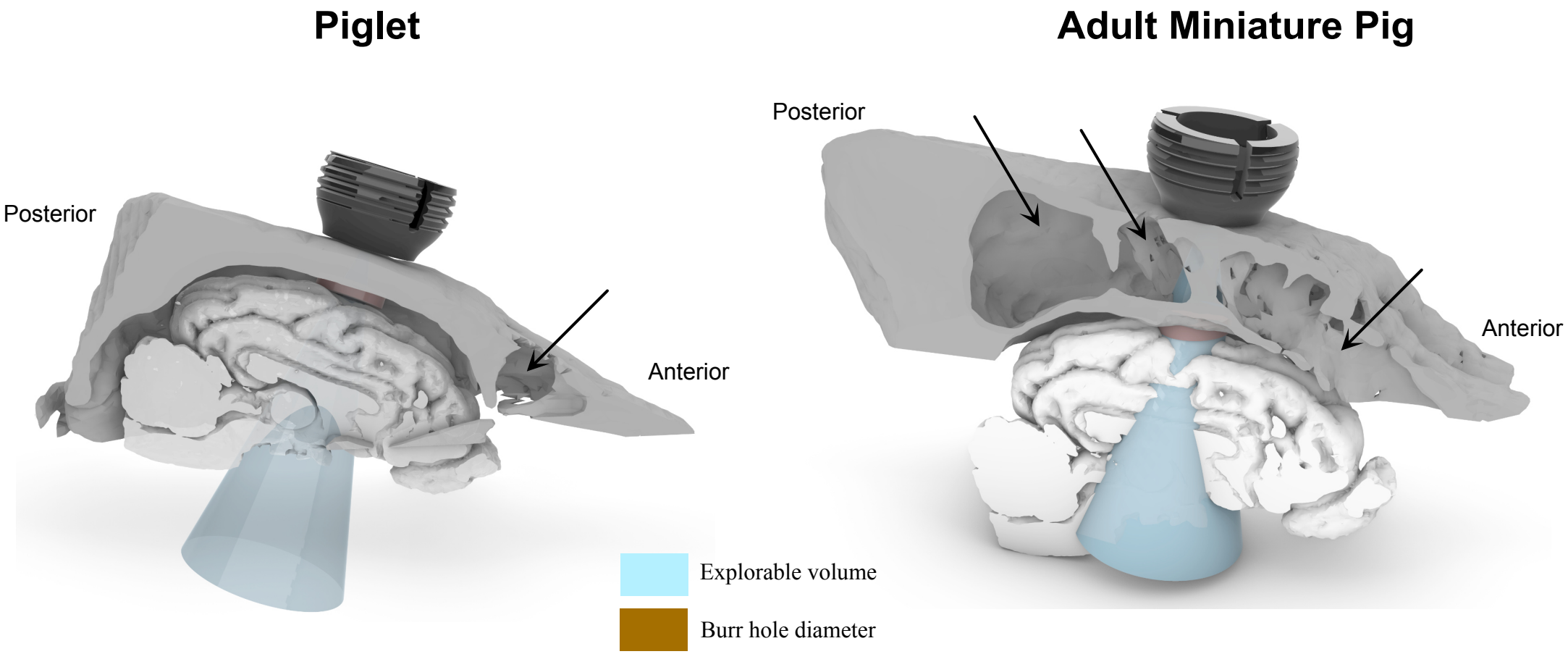
Piglet
Posterior
Anterior
Adult Miniature Pig
Posterior
Anterior
Explorable volume
Burr hole diameter

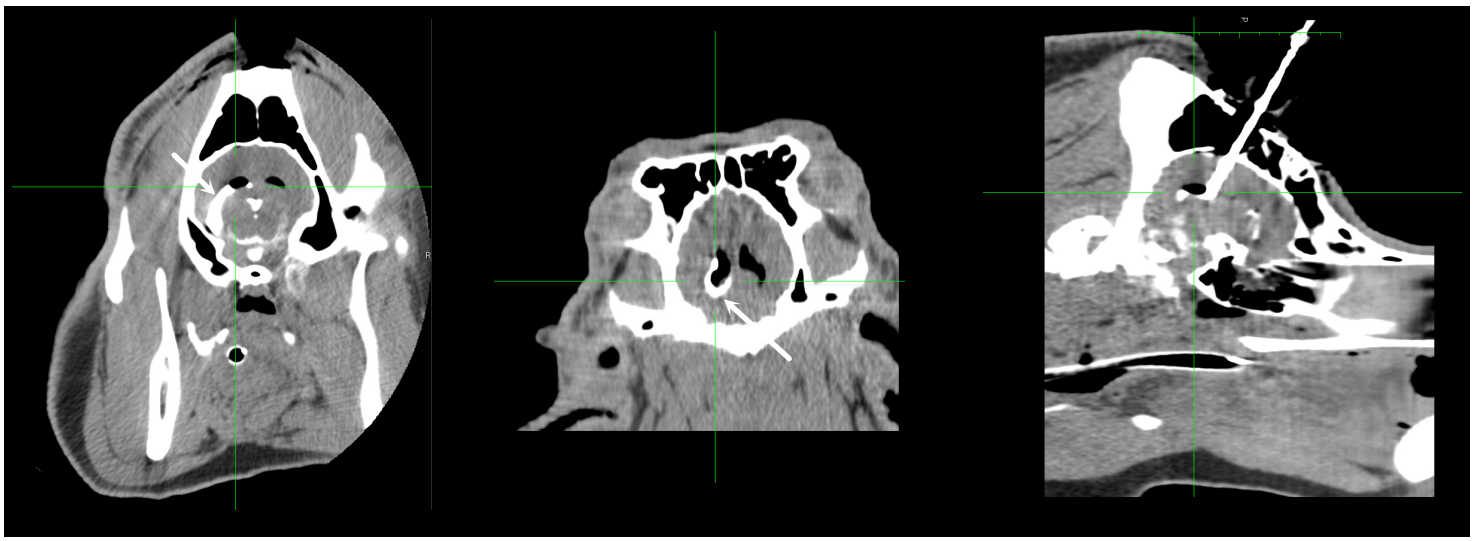

A

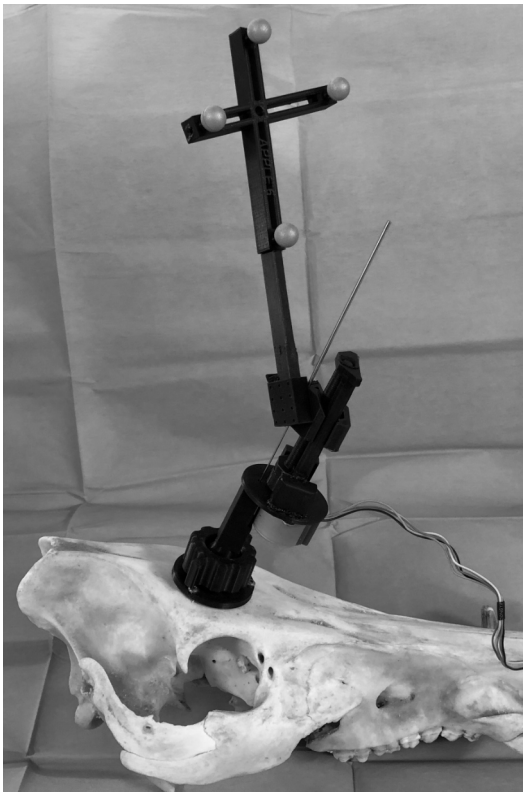

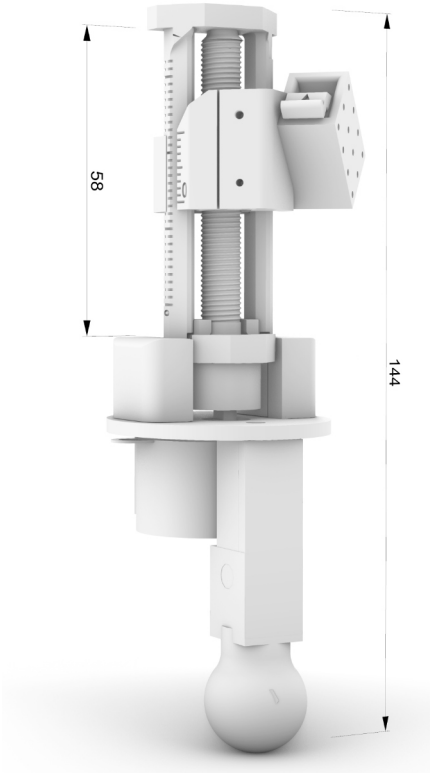

B